Effects of quantum well design on the optical and microwave performance of strained-layer GaInAs/GaAs lasers

S. S. O'Keefe, L. F. Lester, D. Teng, W. J. Schaff, and L. F. Eastman

School of Electrical Engineering and the National Nanofabrication Facility
Cornell University, 424 Phillips Hall, Ithaca, NY 14853 USA

ABSTRACT

By introducing strain into semiconductor lasers using GaAs/$Ga_{1-x}In_xAs$ quantum wells, their modulation bandwidth has been increased to beyond 20 GHz[1,2,3,4]. Our approach to high modulation bandwidth strained layer quantum well lasers has been to fabricate short cavity (less than 100μm) multiple quantum well structures. In order to fabricate lasers of this length, the facets must be etched by chemically assisted ion beam etching (CAIBE) and not by cleaving. In short cavity, multiple strained quantum well lasers fabricated by CAIBE, it has recently been shown using two different layer structures[5,6] that a 3dB modulation bandwidth of 28 GHz is obtainable under cw conditions.

The current study investigates three issues in the fabrication of strained layer quantum well lasers for high speed operation (1) the growth of different quantum well and barrier materials and their effects on device performance, (2) the dependence of differential gain and damping on quantum well width, depth, and number, and (3) the relationship between threshold current (J_{th}) and high speed performance. Wafers have been grown with indium contents from 20 - 40%, well widths from 30 - 70Å, and from two to five quantum wells. From the results on these wafers, some design criteria for optimizing high-speed performance will be presented.

INTRODUCTION

Strained layer semiconductor lasers have shown promise for use in high speed applications by recently attaining 3dB bandwidths of up to 28GHz[5,6], but there are still many questions to be answered about what is the best layer structure for high speed operation. With the many variables of the number of quantum wells(QW), their composition, their barriers (and thus their well depth), and confinement structures, there should be some guidelines about what types of structures give good high speed performance. The goal of this study was to learn about these parameters by comparing the results of many (seven) different wafer structures using equivalent processing on all of the wafers. The results show that high differential gains of up to $2.1x10^{-15}cm^2$ in a 50Å $Ga_{0.7}In_{0.3}As$ 5QW 200μm laser are possible in multiple quantum well (MQW) lasers, but also that high bandwidths are due to deep, wide quantum wells and short carrier capture times[7] as observed in a device with a 3dB bandwidth of 28GHz on a 3QW 70Å $Ga_{0.8}In_{0.2}As$/ $Al_{0.15}Ga_{0.85}As$ wafer. Results from the high speed modulation response of several types of strained quantum well lasers are presented, and comparisons will be made based on the width, depth, and number of these wells. General observations about their response characteristics will be made and guidelines for an optimum high speed device will be discussed.

0-8194-0868-9/92/$4.00

MATERIALS AND FABRICATION

Seven wafer structures were chosen to show the effects of quantum well and confinement structure design on device performance. The effect of the confining structure on the high frequency response of these lasers was investigated by growing similar quantum well structures within a graded index separate confinement heterostructure (GRINSCH) and a simple separate confinement heterostructure (SCH). (See Figure 1 for representative GRINSCH and SCH layer structures.) The first two wafers were 4QW and 5QW GRINSCH lasers and consisted of the following layers: a 1μm n^+-GaAs buffer, a 1500Å n^+-region graded linearly from GaAs to $Al_{0.7}Ga_{0.3}As$, a 4500Å n-$Al_{0.7}Ga_{0.3}As$ cladding region, an undoped 2500Å GRIN region graded linearly from $Al_{0.7}Ga_{0.3}As$ to $Al_{0.3}Ga_{0.7}As$, an active region consisting of 4 (or 5) 50Å $Ga_{0.7}In_{0.3}As$ quantum wells each surrounded by a 250Å undoped GaAs barrier, an undoped 2500Å GRIN region graded linearly from $Al_{0.3}Ga_{0.7}As$ to $Al_{0.7}Ga_{0.3}As$, a 4500Å p-$Al_{0.7}Ga_{0.3}As$ clad region, a 1500Å p^+ region graded linearly from $Al_{0.7}Ga_{0.3}As$ to GaAs, and a 1000Å p^+-GaAs cap.

The other five wafers grown had SCH type cladding structures. The SCH consisted of a 1μm n^+-GaAs buffer, a 1500Å n^+ region graded linearly from GaAs to $Al_{0.7}Ga_{0.3}As$, an 8100Å n-$Al_{0.7}Ga_{0.3}As$ cladding region, a 2000Å confinement region consisting of the quantum wells and their barrier layers, then an 8100Å p-$Al_{0.7}Ga_{0.3}As$ cladding region, a 1500Å p^+ region graded linearly from $Al_{0.7}Ga_{0.3}As$ to GaAs, and a 1200Å p^+-GaAs cap. The quantum wells were centered within the confinement region and the balance of the 2000Å consisted of the respective barrier material. Three wafers with three quantum wells were grown to examine the effect of differences in well thickness and valence band hole-confining well depths on differential gain and damping. Well thicknesses of 35, 50, and 70Å and valence band well depths of 118 and ~150meV were chosen. Also, 2QW and 4QW wafers were grown with 50Å wells (matching the wells in the 3QW wafer) so that trends with respect to the number of quantum wells could be measured. Table 1 shows a summary of the quantum well composition, thickness, and barrier materials for the five SCH wafers.

Table 1 SCH Quantum Wells and Barriers

Wafer Number	# of Wells	Indium Composition in the Well	Quantum Well Width	Barrier Material
4008	3	20%	70Å	$Al_{0.15}Ga_{0.85}As$
4001	3	30%	50Å	GaAs
4002	3	40%	35Å	GaAs
4006	2	30%	50Å	GaAs
4007	4	30%	50Å	GaAs

These wafers were processed into ridge waveguide structures using electron beam lithography and chemically assisted ion beam etching (CAIBE) in a procedure that was been shown in the past to give reproducible, reliable devices[8]. The ridges were etched to a depth of approximately 8000Å in the SCH case and to the top of the undoped graded index region in the GRINSCH wafers. Optical waveguide calculations have shown that these etch depths give the optimum lateral confinement at low power operation, but single mode operation was not

guaranteed for all operating conditions. The mirror/mesa etch stopped nominally at the top of the n^+-GaAs layer to optimize the contact. The n- and p-type contacts were created using Ni/AuGe/Ag/Au and Ti/Pd/Au metallizations respectively while only the n-type contact was annealed. The p-type contact was made only as large as the ridge, either three or five microns wide and 50 to 400 μm long depending upon the size of the device, in order to reduce the excess capacitance associated a large pad while assuming that the inductance of the small metal line was not too large. The laser is flanked by two metallized ground mesas in order to make it compatible with a coplanar waveguide probe (See Figure 2), thus the parasitics associated with bonding are avoided and small (3μm wide) ridges can be contacted directly[9]. The 50Å $Ga_{0.7}In_{0.3}As$ quantum wells typically emit at a wavelength of 1.02μm.

The microwave response curves were measured using an HP 8510B Network Analyzer from 45MHz to 26.5GHz and a New Focus model 1012 long-wavelength photodetector that has a 40 GHz bandwidth. Figure 3 shows a schematic of the microwave setup.

RATE EQUATIONS AND BACKGROUND

In accordance with well barrier hole burning theory, the single mode rate equations that govern the operation of short-cavity ridge waveguide quantum well lasers have the following form[7]

$$\frac{dN_b}{dt} = \frac{I}{e} - \frac{N_b}{\tau_s} - \frac{N_b}{\tau_{cap}} + \frac{N_w}{\tau_e} \tag{1}$$

$$\frac{dN_w}{dt} = \frac{N_b}{\tau_{cap}} - \frac{N_w}{\tau_e} - \frac{N_w}{\tau_s} - v_g G V S \tag{2}$$

$$\frac{dS}{dt} = G v_g \Gamma V S - \frac{S}{\tau_p} \tag{3}$$

where N_b is the number of carriers in the barrier, N_w is the number of carriers in the well, I is the injected current, S is the photon density, G is the gain, V is the quantum well volume, Γ is the confinement factor, v_g is the group velocity, and τ_s, τ_{cap}, τ_e, and τ_p are the recombination, capture, emission, and photon lifetimes respectively. Equations (2) and (3) are consistent with the conventional form of the rate equations, while equation (1) is included to account for the population of carriers in the barrier regions. Justification for the use of this set of rate equations is discussed later. Using small signal analysis on equations (1)-(3), one obtains the following characteristic modulation response

$$|R|^2 = \frac{1}{1 + \omega^2 \tau_{cap}^2} \frac{\omega_o^4}{(\omega^2 - \omega_o^2)^2 + \omega^2 \gamma^2} \tag{4}$$

$$\omega_o^2 = \frac{v_g\, g_n\, S_o}{\sigma \tau_p} \tag{5}$$

$$\gamma = \frac{1}{\sigma \tau_s} + \omega_o^2 \tau_p + \frac{1}{\sigma \tau_e} \frac{\omega^2 \tau_{cap}^2}{\left(1 + \omega^2 \tau_{cap}^2\right)} \tag{6}$$

$$\sigma = 1 + \frac{\tau_{cap}/\tau_e}{(1 + \omega^2 \tau_{cap}^2)} \tag{7}$$

where ω_o is the resonance frequency, γ is the damping rate, and g_n is the differential gain. Equation (4) takes the form of the ideal laser response, but is modified by a term equivalent to a low pass filter that depends upon the capture time of carriers into the well. The low frequency rolloff was observed in our devices and our microwave response curves could be fit this equation to extract the values of τ_{cap}, ω_o, and γ.

The figures of merit for highest speed operation in these devices are a small carrier capture time, a high differential gain, and a low damping rate. The slope of the line fitted to the square of the relaxation oscillation frequency with the bias current above threshold was used to calculate the differential gain of the various lasers according to the equation

$$g_n = \frac{4\pi^2 e W d L}{\eta_i v_g \Gamma} \frac{f_0^2}{\left(I - I_{th}\right)} \tag{8}$$

where W is the ridge width, L is the cavity length, d is the active region thickness, η_i is the internal quantum efficiency, v_g is the group velocity, Γ is the optical confinement factor, f_o is the resonance frequency, and $(I-I_{th})$ is the current level above threshold. Using the conventional rate equations, γ takes the form of

$$\gamma = \frac{1}{\tau_s} + K \omega_o^2 \tag{8}$$

where the K-factor has units of time. At the frequencies of interest, the first term in equation (8) is negligible and is typically ignored. At high photon densities, it is common to simulate gain suppression using a non-linear gain coefficient, ε. By substituting a modified gain, $g = g/(1+\varepsilon S)$, into equations (1)-(3), and again solving for the small signal response, ε takes on the following form

$$\varepsilon = g_n \left(\frac{K v_g}{4\pi^2} - \frac{1}{\alpha_t} \right) \tag{9}$$

where α_t is the total cavity loss. This non-linear gain coefficient is calculated from the K-factor (γ/f_0^2) at maximum bandwidth. Although ε is a common figure of merit to describe damping, a more direct measure of the damping is a low K-factor at maximum bandwidth.

RESULTS AND DISCUSSION

There were several observations made about the growth of strained layer quantum well lasers during this study. To study the effect of a large heterojunction offset for a quantum well with low indium content, wafer #4008 with three 70Å $Ga_{0.8}In_{0.2}As$ wells and $Al_{0.15}Ga_{0.85}As$ barriers was grown. The difficulty involved in using this layer structure is that it is hard to grow optical quality $Al_{0.15}Ga_{0.85}As$ and even harder to grow good quality $Ga_{0.8}In_{0.2}As$ directly on this $Al_{0.15}Ga_{0.85}As$. Usually lasers with Al in the wells or in the confinement regions have high thresholds, but through the use of smoothing layers in the cladding regions, growth stops during the quantum well growth, and careful control of substrate temperatures, a wafer with low thresholds (10.4mA versus 8.2mA on a similar device from wafer #4001), good microwave properties, and a record bandwidth on a 3QW laser of 28GHz with g_n of $1.4x10^{-15}cm^2$ was obtained. Differential gain and bandwidth results have recently been published on similar devices with an active region that consisted of three 70Å $Ga_{0.8}In_{0.2}As$ wells surrounded by GaAs barriers and a similar confinement structure[10]. A correction must be made in their conversion from output power to photon density, though, to account for the distributed nature of the light wave at the mirror. Converting their g_n of $6.4x10^{-15}cm^2$ on a 500μm long device to our method of calculation and using a mirror reflectivity of 0.32, a value for g_n of $1.1x10^{-15}cm^2$ is obtained. A smaller laser should have a smaller g_n, but due to an increased heterojunction offset in the quantum wells, a larger g_n of $1.4x10^{-15}cm^2$ was obtained on our 100μm devices. This device demonstrates the possibility of using AlGaAs as a quantum well barrier material for strained layer MQW lasers, allowing deep quantum wells to be fabricated without the need for a high indium content well material.

To obtain the same valence band offset (ΔEv) as in wafer #4008 without the AlGaAs barriers, highly strained (2.9%) $Ga_{0.6}In_{0.4}As$ wells are required, limiting the quantum well thickness to 35Å in a three quantum well wafer due to critical layer thickness considerations[11]. Wafer #4002 was grown with this well design. Comparing lasers from this wafer to #4008, we observed that the maximum bandwidth of 23GHz and the g_n of $1.2x10^{-15}cm^2$ were both lower on the wafer with thin wells. This result and the values of the K-factor shown in Table 2 prompt the conclusion that the barrier height is not the only important design parameter for quantum wells, but that the well width must also be considered.

Table 2. Material parameters and device results of the SCH wafers on $100x3\mu m^2$ devices

# of Wells	Indium Composition	Quantum Well Width	Barrier Material	Valence Well Depth (meV)	Differential gain (cm^2)	K-Factor at max ω_o (nsec)
3	20%	70Å	$Al_{0.15}Ga_{0.85}As$	150	$1.4x10^{-15}$	0.10
3	30%	50Å	GaAs	118	$0.8x10^{-16}$	0.11
3	40%	35Å	GaAs	156	$1.2x10^{-15}$	0.15
2	30%	50Å	GaAs	118	$4.0x10^{-16}$	0.17
4	30%	50Å	GaAs	118	$1.0x10^{-15}$	0.08

The two well-known ways to make a faster laser are to avoid the phenomenon of gain saturation with current density by increasing the number of wells and to reduce the photon lifetime by reducing the cavity length. By increasing the number of quantum wells to four in the case of 30% indium wells, a 28 GHz bandwidth result on a $3x150\mu m^2$ device was obtained, but the shorter devices all had worse microwave performances. The only 50μm devices that worked were on the 5QW wafer, while the 100μm 4QW GRINSCH wafer has a maximum 3dB bandwidth of only 26GHz. We believe that in smaller devices, higher carrier densities associated with higher losses lead to a larger increase in the damping factor than in long devices. At low carrier densities the quasi-fermi level is pinned and is in the wells, but at very high injection levels carrier heating occurs and the quasi-fermi level rises, lessening the confining potential of the well. Since thermionic emission out of a well is proportional to the exponential of the barrier height, we expect the turn-on of this phenomenon to be observed as a rather abrupt decrease in the τ_e. In short cavity SCH lasers with a short capture time, σ in equation (8) reduces to $1+\tau_{cap}/\tau_e$ while the damping coefficient, γ, becomes

$$\gamma = \omega_o^2\left(\tau_p + \frac{\tau_{cap}^2}{\tau_e + \tau_{cap}}\right) \tag{10}$$

Thus a decrease in τ_e results in an increase in the damping at high current levels as shown in Figure 5 in 4 and 5QW SCH and GRINSCH devices. We believe that this effect is the cause of the lower maximum frequency response in the thin 40% indium wells. A thin well results in a lower 2D density of states so the increase in the quasi Fermi level will be more pronounced. No increase in the τ_{cap} was measured in the microwave results at high power because the capture time is related more to the structure of the confining region than to the carrier density or the wells.

There was also a difference in the measured low frequency rolloffs of the GRINSCH and SCH devices. The dip in the microwave response was more pronounced in the case of the GRINSCH as can be seen in Figure 4. Using equation (4) it was possible to extract τ_{cap} from these plots. The GRINSCH structure had a τ_{cap} of 72ps, corresponding to a pole frequency of 10GHz, while the SCH device had a τ_{cap} of only 18ps, placing its pole at a more reasonable 50GHz. This low frequency pole is, to a large degree, what was limiting the frequency response of the GRINSCH devices.

In the past, low threshold buried heterostructure lasers have been targeted for high speed applications, but the parasitic capacitances of the carrier-confining junctions greatly hinder their high speed performance. We propose the viability of ridge waveguide structures in these applications because of the lack of a regrowth step, greatly reduced parasitics, and relative ease in processing. Even though there are large leakage currents associated with ridge lasers, it does not seem to be a hindrance to their operation. In comparing $3x100\mu m^2$ device thresholds in the 2, 3, and 4QW 50Å quantum well wafers, it was found that the 2QW devices had only slightly lower threshold currents (~7mA) than both the 3 and 4QW devices (8-9mA). Since leakage current was such a major part of the drive current, fewer quantum wells did not reduce I_{th} enough to affect the difference $(I-I_{th})$ at high drive currents.

CONCLUSION

The microwave response of several strained layer multiple quantum well lasers were analyzed to try to determine the best set of design parameters for the active region and confining structure. Consistent with the theory of well-barrier hole burning, the best results occurred in a 3QW device with wide, deep wells consisting of 70Å $Ga_{0.8}In_{0.2}As$ wells with $Al_{0.15}Ga_{0.85}As$

barriers. The series of 2, 3, and 4QW 50Å $Ga_{0.7}In_{0.3}As$ devices showed that increasing the number of wells also increases performance and that in ridge waveguide structures, leakage currents minimize the expected lowering of I_{th} in the 2QW device. The low-frequency rolloff that has been observed in all of these devices is less pronounced in SCH type devices than in the GRINSCH material. We thus propose that a laser with high differential gain, lower high frequency damping, and a higher 3dB bandwidth will be produced if a short-cavity device is produced on material with as many wide, deep quantum wells as is possible within the limits of critical layer thickness considerations using an SCH type confinement structure.

ACKNOWLEDGMENT

The authors would like to thank John Bowers, Radhakrishnan Nagarajan, and Wayne Sharfin for many useful discussions. This work was supported by ONR under contract #N00014-89-J-11386 with additional support from GE, IBM, and DARPA.

REFERENCES

1. I. Suemune, L. A. Coldren, M. Yamanishi, and Y. Kan, "Extremely wide modulation bandwidth in a low threshold current strained quantum well laser," *Appl. Phys. Lett.*, vol. 53, pp. 1378-1380, 1988.
2. S. D. Offsey, W. J. Schaff, P. J. Tasker, and L. F. Eastman, "Optical and microwave performance of GaAs-AlGaAs and strained layer InGaAs-GaAs-AlGaAs graded index separate confinement heterostructure single quantum well lasers," *Photonics Tech. Lett.*, vol. 2, pp. 9-11, 1990.
3. R. Nagarajan, T. Fukushima, J. E. Bowers, R. S. Geels, and L. A. Coldren, "High-speed InGaAs/GaAs strained multiple quantum well lasers with low damping," *Appl. Phys. Lett.*, vol. 58, no. 21, pp. 2326-2328, 1991.
4. L. F. Lester, W. J. Schaff, X. Song, L. F. Eastman, "Optical and RF characteristics of short-cavity-length multiquantum-well strained-layer lasers," *Photonics Tech. Lett.*, to be published Dec. 1991.
5. L. F. Lester, S. S. O'Keefe, W. J. Schaff, and L. F. Eastman, "Multiquantum well strained-layer lasers with improved low frequancy response and very low damping," *Electronics Letters*, vol. 28, no. 4, pp. 383-385, 1992.
6. L.F. Lester, D. Teng, W.J. Schaff, and L.F. Eastman, "Design of quantum well lasrs forhgh differential gain," *Leos '91 Conference Digestt*, San Jose, Ca., 1991.
7. W. Rideout, W. F. Sharfin, E. S. Koteles, M. O. Vassell, and B. Elman, "Well-barrier hole burning in quantum well lasers," *IEEE Photon. Technol. Lett.*, vol. 3, pp. 784-786, 1991.
8. L. F. Lester, W. J. Schaff, S. D. Offsey, and L. F. Eastman, "High-speed modulation of InGaAs-GaAs strained-layer multiple-quantum-well lasers fabricated by chemically assisted ion-beam etching," *IEEE Photon. Technol. Lett.*, vol. 3, pp. 403-405, 1991.
9. S. D. Offsey, W. J. Schaff, P. J. Tasker, and L. F. Eastman, "Optical and microwave performance of GaAs-AlGaAs and strained layer InGaAs-GaAs-AlGaAs graded index separate confinement heterostructure single quantum well lasers," *IEEE Photon. Technol. Lett.*, vol. 2, pp.9-11, 1990.
10. N.K. Dutta, J. Lopata, D.L. Sivco, and A.Y. Cho, "High-speed modulation and nonlinear damping effect in InGaAs/GaAs lasers," *J. Appl. Phys*, vol. 70, no. 4, pp. 2476-2478, 1991.
11. J.W. Matthews and A.E. Blakeslee, "Defects in epitaxial multilayers, I. Misfit Dislocations," *J. of Crystal Growth*, vol. 27, pp. 118-125, 1974.

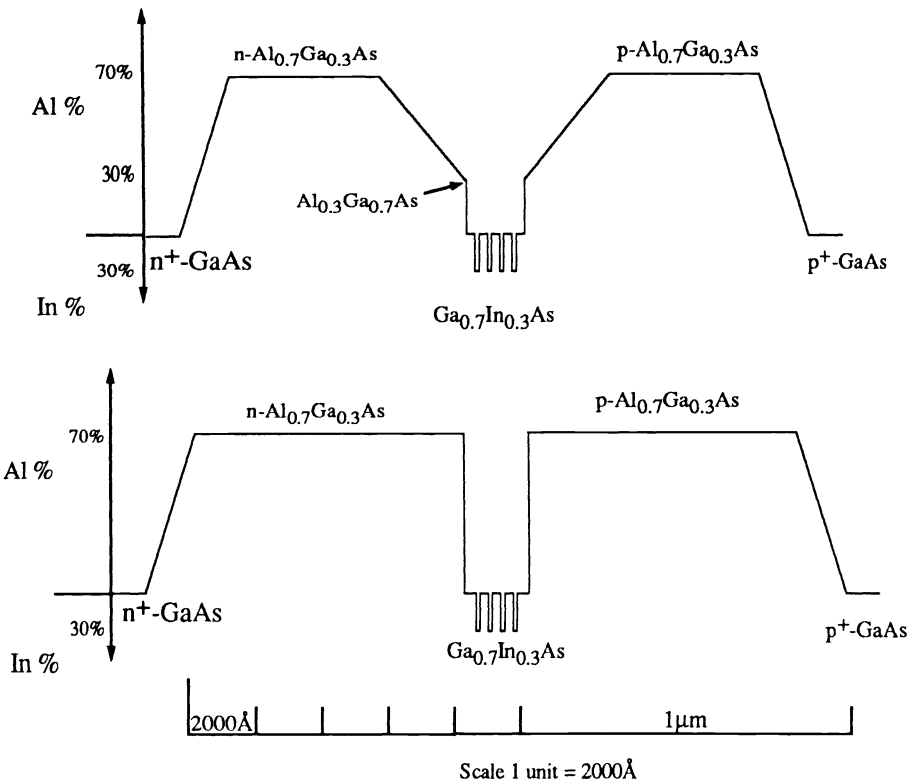

Figure 1 GRINSCH and SCH wafer design

Figure 2 Cascade probe and laser

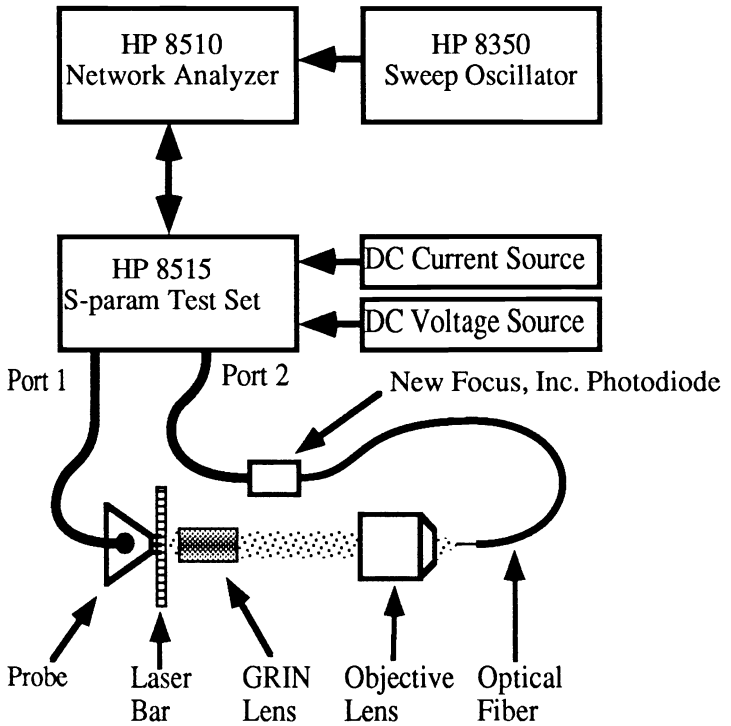

Figure 3 Microwave setup

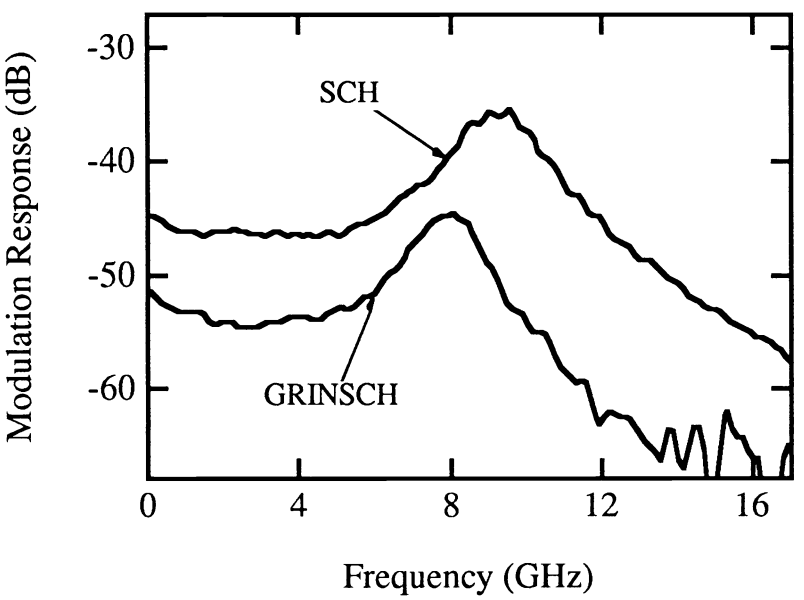

Figure 4 A comparison of the modulation responses of the 4QW GRINSCH and SCH 100 x 3 μm lasers

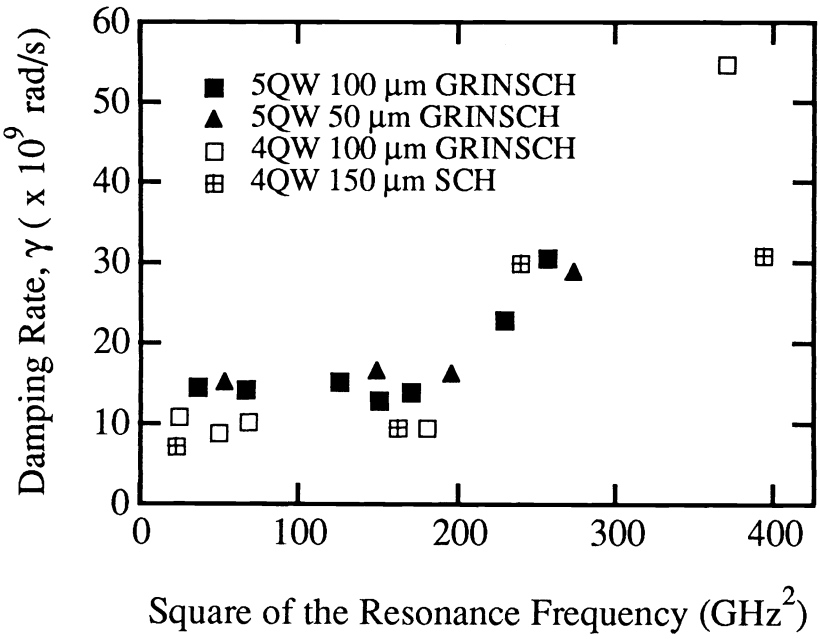

Figure 5 A graph of the damping rate as a function of the square of the resonance frequency for various short cavity GRINSCH lasers and the high bandwidth 4QW SCH laser.